


Article

Structure and Properties of Highly Porous Alumina-Based Ceramic Materials after Heating by Concentrated Solar Radiation

Vladimir G. Babashov ^{1,*}, Sultan Kh. Suleimanov ² , Mikhail I. Daskovskii ¹, Evgeny A. Shein ¹ and Yurii V. Stolyankov ¹

¹ NRC “Kurchatov Institute”-VIAM, 105005 Moscow, Russia; daskovskiy@gmail.com (M.I.D.); sheinea@rambler.ru (E.A.S.); stolyankov@mail.ru (Y.V.S.)

² Physical-Technical Institute of SPA “Physics-Sun”, Academy of Sciences of the Republic of Uzbekistan, Tashkent 100084, Uzbekistan; sultan.suleimanov@gmail.com

* Correspondence: inno@viam.ru

Abstract: Three ceramic fibrous materials of the Al_2O_3 - SiO_2 system with different densities have been treated using concentrated solar radiation. The experiment was performed using technological capabilities of the Big Solar Furnace in the 2 modes: the first mode includes heating up to 1400–1600 °C, holding for 1.5–2 h; the second mode (the fusion mode) includes heating up to 1750–1900 °C until the sample destruction, which is accompanied by fusion. Upon completion of the experiment, the phase composition, microstructure, and compressive strength of the materials were studied. It was shown that the investigated materials retained their fibrous structure under prolonged treatment in the first mode up to temperatures of 1600 °C. The phase composition of the ceramic materials changes during the experiment, and with a decrease in the density, the modification is more pronounced. Treatment of all three materials under study in the fusion mode resulted in the formation of the eutectic component in the form of spherulites. The compressive strength of the materials was found to be slightly reduced after exposure to concentrated solar radiation.

Keywords: highly porous ceramic materials; Al_2O_3 - SiO_2 system; concentrated solar radiation; microstructure; phase composition



Citation: Babashov, V.G.; Suleimanov, S.Kh.; Daskovskii, M.I.; Shein, E.A.; Stolyankov, Y.V. Structure and Properties of Highly Porous Alumina-Based Ceramic Materials after Heating by Concentrated Solar Radiation. *Ceramics* **2022**, *5*, 24–33. <https://doi.org/10.3390/ceramics5010003>

Academic Editor: Cristina Siligardi

Received: 23 November 2021

Accepted: 28 December 2021

Published: 30 December 2021

Publisher’s Note: MDPI stays neutral with regard to jurisdictional claims in published maps and institutional affiliations.



Copyright: © 2021 by the authors. Licensee MDPI, Basel, Switzerland. This article is an open access article distributed under the terms and conditions of the Creative Commons Attribution (CC BY) license (<https://creativecommons.org/licenses/by/4.0/>).

1. Introduction

The development of high-temperature heat-insulating materials based on oxide fibers is the actual worldwide line of inquiry. The application of refractory oxide fibers as precursors of heat-insulating materials are favored due to their exceptional oxidation resistance at temperatures above 1200 °C, chemical inertness with respect to most substances, and low density. Ceramic refractory materials based on the Al_2O_3 - SiO_2 system are widely used as heat-insulating materials. According to [1], the structure of the material based on the Al_2O_3 - SiO_2 system contains solid non-fibrous inclusions, which have a negative effect on the material properties during long-term operation at high temperatures, especially under cyclic loading. Referring to [2], mullite fiber-reinforced Al_2O_3 - SiO_2 aerogel composite obtained using hybrid sol-gel process has excellent heat-insulating characteristics, high-temperature stability, and high mechanical properties. Here, mullite fiber increases the material strength, while the unique porous structure ensures good heat-insulation properties. The heat resistance of the Al_2O_3 aerogel- SiO_2 fiber composite [3,4] is ensured by the formation of a crystal structure based on the γ - Al_2O_3 and δ - Al_2O_3 phases. According to [5], Al_2O_3 - SiO_2 ceramics can be produced by combination of silica-sol infiltration and Selective Laser Sintering (SLS). The phase composition of this material is represented by mullite, quartz, corundum, and cristobalite. With an increase in the amount of silica sol, the amount of cristobalite in the structure of the material increases, which avoids excessive shrinkage

during the sintering process. As is shown in [6], with an increase in the content of silica sol and the sintering temperature up to 1300 °C, the compressive strength of SiO₂/Al₂O₃-SiO₂ fiber mat composite increases from 0.3 to 0.9 MPa, and the density increases from 0.25 to 0.45 g/cm³. The structure of the composite material sintered at 1300–1400 °C contains mullite and cristobalite.

It should be noted that the behavior of such materials under conditions of high-speed “sudden” heating remains insufficiently studied. One of the effective methods of high-speed heating is the exposure to concentrated solar radiation, implemented in the design of the Big Solar Furnace [7]. The Big Solar Furnace allows testing porous ceramic materials and heating up to ~2000 °C [8–10].

Of special interest is the study of changes in the phase composition of highly porous fibrous ceramic materials during long-term high-temperature treatment. Materials of different density based on the same fiber type can be used at different operating temperatures. It was shown that materials with a relatively high density had lower values of the thermal conductivity at temperatures above 1200 °C, while materials with a lower density had low values of thermal conductivity at temperatures below 900 °C [11].

In addition, the effect of concentrated solar radiation on the surface of a ceramic material is of interest. A promising method of processing is the surface treatment of Al₂O₃-based ceramics with laser radiation, which makes it possible to form a modified layer with a phase composition that differs from that of the underlying layers [12].

This work deals with the investigation of Al₂O₃-SiO₂ ceramic fibrous materials with different densities after heat treatment through concentrated solar radiation. The presented study may give a clearer insight into the behavior of ceramic fibrous materials based on the Al₂O₃-SiO₂ system under conditions of high-speed “sudden” heating realized at the Big Solar Furnace. The data obtained during the experiment at the Big Solar Furnace may be used, for example, to evaluate the applicability of the materials under study as components of thermal protection systems for flight vehicles. In addition, the experiments using the Big Solar Furnace may allow elaborating the methods of testing ceramic materials, as well as the methods for preparation of new materials and chemical compounds with unique properties.

2. Materials and Methods

A total of 3 ceramic composite materials of the Al₂O₃-SiO₂ system with different densities (the material I—1000 kg/m³, the material II—500 kg/m³, the material III—300 kg/m³) were selected for this study. These materials contain discontinuous fibers with a composition of 80% Al₂O₃ + 20% SiO₂ as a basis. The materials I, II were obtained using molding with a binder followed by firing. Quartz (SiO₂) microfibers and boron were used as a binder for the materials I, II. A solution of aluminum nitrate and a colloidal solution of silicon dioxide were used as a binder for the material III. The fibrous blocks were formed on a vacuum unit using the following procedure: a solid-phase binder was added to the fibrous pulp (the materials I, II); a dry fibrous block was impregnated with a liquid-phase binder (the material III). Then, the materials were dried and subjected to high-temperature heat treatment. To conduct the experiment, samples of these 3 materials were made in the form of blocks with dimensions of 100 × 100 × 40 mm. The properties of the materials under study are shown in Table 1. The microstructure of the materials under study is depicted in Figure 1.

High-temperature treatment of ceramic materials was carried out using a unique facility—the Big Solar Furnace located in the Republic of Uzbekistan (Parkent city), which was put into operation in 1987 [13–15] (Figure 2). The samples of 3 materials were installed in a fixture and exposed to 1-sided heating by means of concentrated solar radiation with a flux density of 730–925 W/m² (Figure 3). The temperature from the front side of the samples was monitored using a KTX (Heitronics Infrarot Messtechnik GmbH, Wiesbaden, Germany) optical pyrometer with a wavelength of 7.5–8 μm. In addition, the temperature inside the samples was measured with thermocouples located in the upper, middle,

and lower parts of the samples. The temperature difference between the upper and the lower parts of the samples reached 290 °C. The experiment was carried out in the 2 modes: the first mode includes heating up to 1400–1600 °C, holding for 1.5–2 h; the second mode (the fusion mode) includes heating up to 1750–1900 °C until the sample destruction, which is accompanied by fusion.

Table 1. The properties of three ceramic composite materials under study before the experiment.

	Material I	Material II	Material III
Density, kg/m ³	1000	500	300
Porosity, % vol.	50	80	93
Chemical composition	73%Al ₂ O ₃ -27%SiO ₂	73%Al ₂ O ₃ -27%SiO ₂	75%Al ₂ O ₃ -25%SiO ₂
Phase composition	Mullite (3Al ₂ O ₃ ·2SiO ₂), δ-Al ₂ O ₃	Mullite (3Al ₂ O ₃ ·2SiO ₂), δ-Al ₂ O ₃	Mullite (3Al ₂ O ₃ ·2SiO ₂), δ-Al ₂ O ₃
Thermal conductivity coefficient, W/(m·K)	20 °C–0.27	20 °C–0.11	20 °C–0.07
	1000 °C–0.32	1000 °C–0.25	1000 °C–0.22
	1600 °C–0.51	1600 °C–0.48	1600 °C–0.37

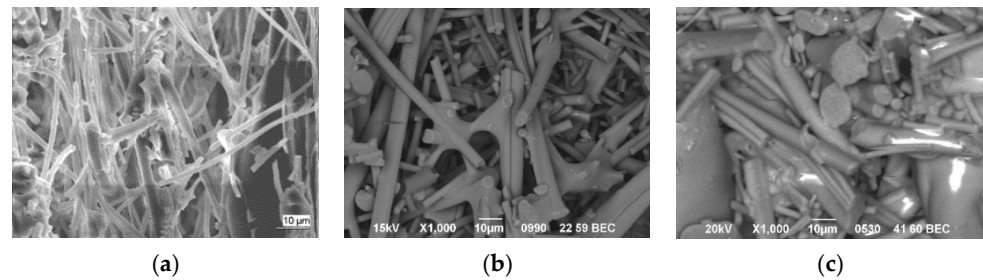


Figure 1. The microstructure of fibrous ceramic materials: (a) The material I; (b) The material II; (c) The material III.

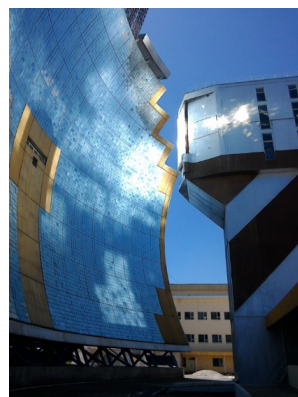


Figure 2. The solar concentrator and the technological tower of the Big Solar Furnace.



Figure 3. The sample of the material II after exposure to concentrated solar radiation.

After high-temperature treatment, the changes in the structure and properties of the samples of the materials I, II, III were investigated. X-ray diffraction analysis was performed using a DRON-3M diffractometer (Cu $K\alpha$ radiation). In case of the first mode, the specimens for analysis were cut both from the “hot” side (solar side) and from the “cold” side of the samples. The microstructure and elemental composition were studied using a Zeiss EVO MA10 (Oxford Instruments, Abingdon, UK) scanning electron microscope equipped with an energy-dispersive spectrometer. The compressive strength of the materials under study was determined using an Instron 5582 tensile tester (Instron, Buckinghamshire, UK).

The work was carried out using the equipment of the Core facility center “Climatic Testing” of the NRC “Kurchatov Institute”-VIAM.

3. Results and Discussion

3.1. Phase Composition

The diffraction pattern taken from the surface of the initial materials (i.e., before exposure to concentrated solar radiation) is represented by high-intensity reflections from mullite ($3Al_2O_3 \cdot 2SiO_2$; PDF #79-1455) and low-intensity reflections from delta-aluminum oxide ($\delta-Al_2O_3$; PDF #79-1455) (Figure 4). The binder is X-ray amorphous, as evidenced by the presence of a small “halo” at 20° . As may be seen from Figure 4, the phase composition of the initial materials (using the material II as an example) is similar to that of the basic fiber.

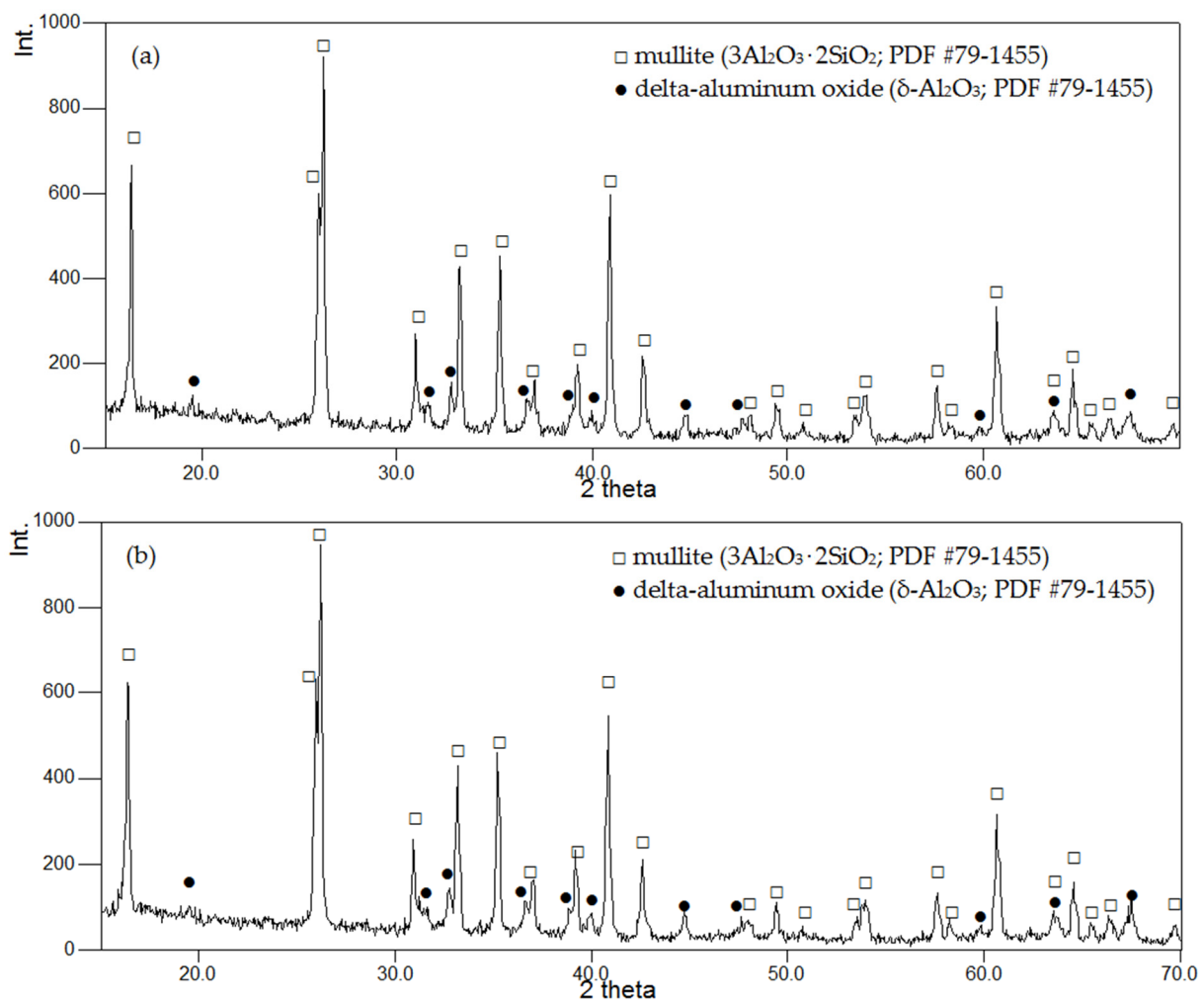


Figure 4. The diffraction pattern of the material II before exposure to concentrated solar radiation (a) as compared with that of the basic fiber [80% Al_2O_3 + 20% SiO_2] (b).

Treatment of the materials with a highly concentrated energy source leads to a change in the phase composition. Reflections from a new phase component, corundum (α - Al_2O_3 ; PDF#46-1212), appear on the diffraction pattern of the treated material I. The diffraction pattern of the specimen cut from the “hot” side shows an increase in the reflections from α - Al_2O_3 and δ - Al_2O_3 in comparison with the specimen taken from the “cold” side. We can say that the amount of the α - Al_2O_3 phase on the “hot” side of the sample is greater than on the “cold” side, since the intensity of the reflection at 35.14° (the reflection from the (104) plane of α - Al_2O_3) significantly increases (Figure 5). At the same time, we can note the formation of more distinct reflections in the region of 67 – 68° , which correspond to δ - Al_2O_3 and α - Al_2O_3 phases. This can be associated both with the transition of the metastable δ - Al_2O_3 to the stable α - Al_2O_3 and with the formation of these phases from mullite during the exposure to concentrated solar radiation.

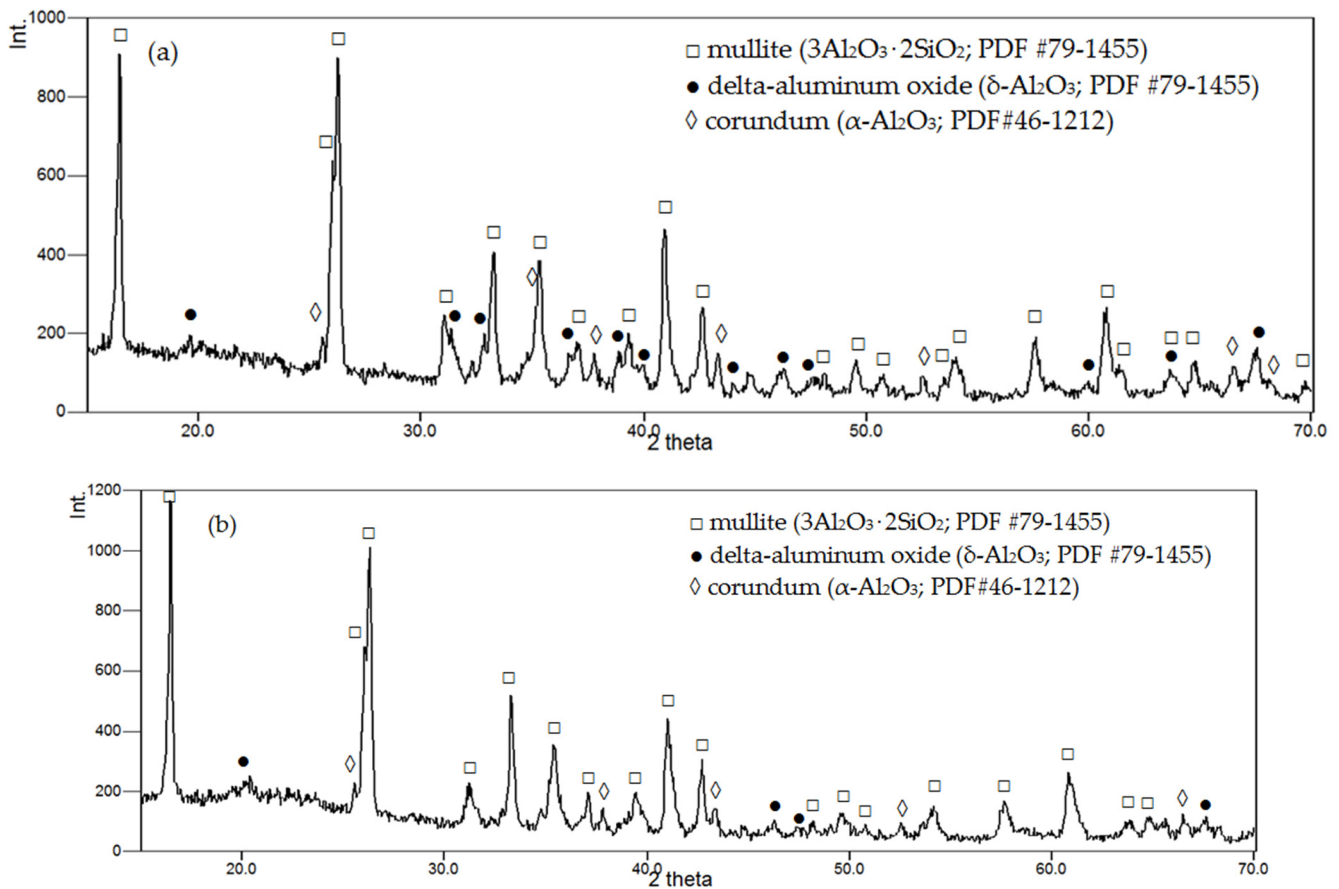


Figure 5. The diffraction pattern of the material I after heating to 1600°C with concentrated solar radiation: the specimen from the “hot” side of the sample treated in the first mode (a); the specimen from the “cold” side of the sample treated in the first mode (b).

In addition to reflections related to corundum, reflections from cristobalite (SiO_2 ; PDF #76-941) appear in the diffraction pattern of the treated material II (Figure 6). The precision data obtained for the powder specimen II indicate the presence of the low-temperature modification of cristobalite. A quantitative assessment by the external standard method gives the following content of phase components: mullite—89%, δ - Al_2O_3 —5%, α - Al_2O_3 —5%, cristobalite—1%.

The diffraction pattern for the treated material III contains reflections from two new phase components—corundum and cristobalite (Figure 7).

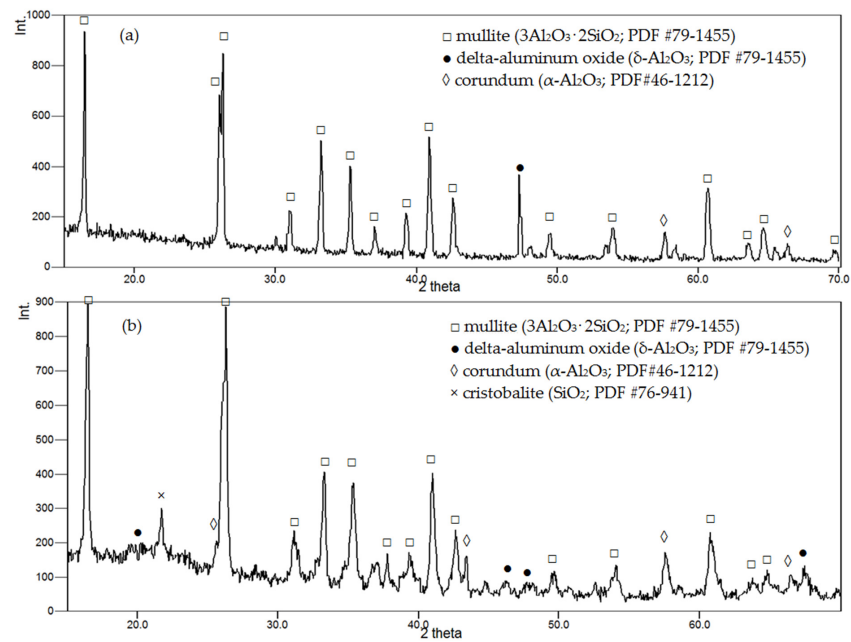


Figure 6. The diffraction pattern of the specimens of the material II after exposure to concentrated solar radiation: the specimen from the sample treated in the fusion mode (a); the specimen from the “cold” side of the sample treated in the first mode (b).

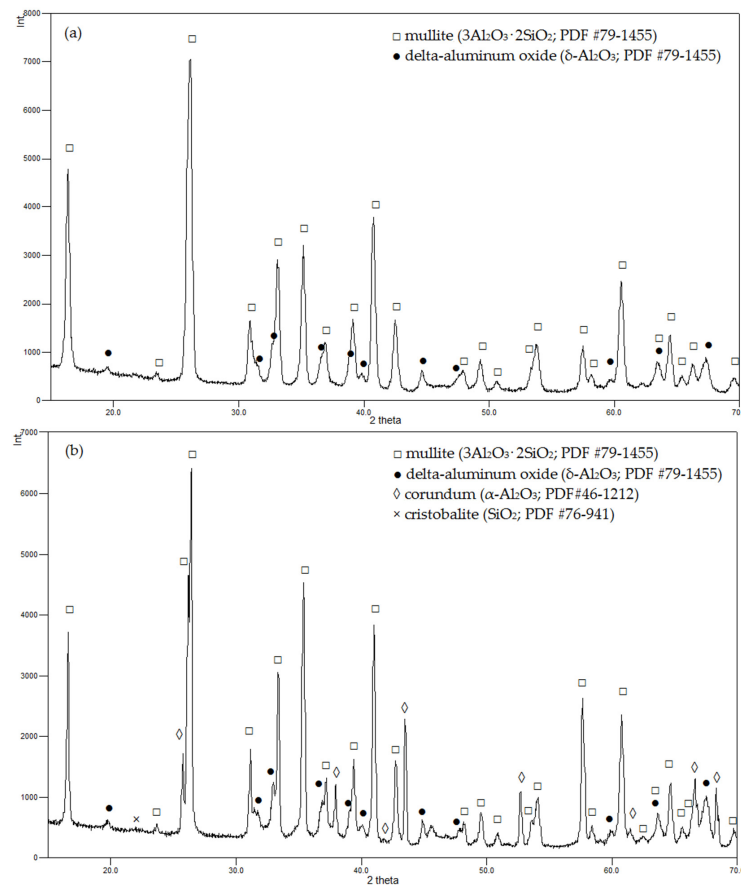


Figure 7. The diffraction pattern of the specimens of the material III after exposure to concentrated solar radiation: the specimen from the “cold” side of the sample treated in the first mode (a); the specimen from the “hot” side of the sample treated in the first mode (b).

As in the case of the material I, an increased amount of α -Al₂O₃ is observed on the surface of the “hot” side samples for the materials II, III.

For all three materials under study, the diffraction pattern of the samples treated in the fusion mode differs from that for the samples treated in the first mode (Figure 6). A reflection of rather high intensity appears near 47°, while some low-intensity reflections disappear. These changes can be associated with the formation of the eutectic component observed in the form of spherulites. One of the possible mechanisms for the formation of the eutectic component during the crystallization of the melt may include changing the initial composition of the Al₂O₃-SiO₂ system to the stoichiometric ratio.

3.2. Microstructure

An investigation of the structure for initial and heat-treated samples was performed by scanning electron microscopy. The structure of the material I is formed by a skeleton of fibers of different diameters. The skeleton fibers have a regular cylindrical shape, with the diameter reaching several tens of micrometers. The inter-fiber space is filled with discrete fibers with a diameter of 1–10 μ m. The elemental composition of large and small fibers does not differ. There are also large spherical buildups. The diameter of the skeleton fibers for the material II is 10–12 μ m, the inter-fiber space is filled with discrete fibers with a diameter of 1–5 μ m. A skeleton of fibers with a diameter of 1–4 μ m forms the structure of the material III.

SEM images of the treated materials are shown in Figure 8 by the example of the material II. Some differences are observed in the structure of the “hot” and the “cold” sides (the first mode of the treatment). The surface layer of the sample from the “hot” side contains a large number of non-fibrous inclusions surrounded by voids. The most probable reasons for the formation of such voids can be the processes of recrystallization and shrinkage of fibers, selective evaporation of individual structural components, as well as the loss of fibers under the influence of energy flow. The thickness of such a layer does not exceed 300 microns. The structure of the sample from the “cold” side has no visible differences from the structure of the initial material; non-fibrous inclusions are practically absent. The morphology of the fiber surface for the “hot” side sample is not fundamentally different from that for the “cold” side sample. In case of the material I, characterized by high density, the difference between the “cold” and the “hot” sides is more pronounced.

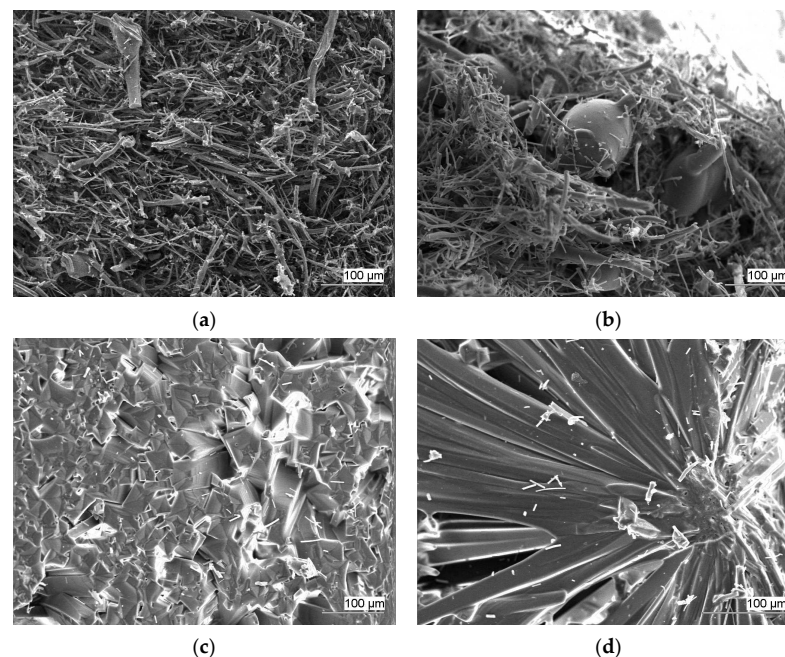


Figure 8. SEM images of the material II after exposure to concentrated solar radiation: (a) the first mode, the “cold” side; (b) the first mode, the “hot” side; (c) the fusion mode; (d) the fusion mode, spherulite.

The microstructure of the samples treated in the second mode (the fusion mode) significantly differs from that of the samples treated in the first mode. Recrystallization of fibers is observed with the formation of non-fibrous particles, sintered into a dense ceramic material, and consisting of cubic crystals with a size of about 10–50 microns. There are also spherulites of 1–2 mm in size, formed by needle-like crystals (see Figure 8d).

3.3. Elemental Composition

The elemental composition of fibers and areas of their connection was studied by the SEM-EDS. For the investigated fibers, regardless of their size, the atomic fraction of aluminum is the highest; oxygen and silicon are also present. Fiber fusion areas contain predominantly silicon and oxygen, as well as aluminum (Figure 9).

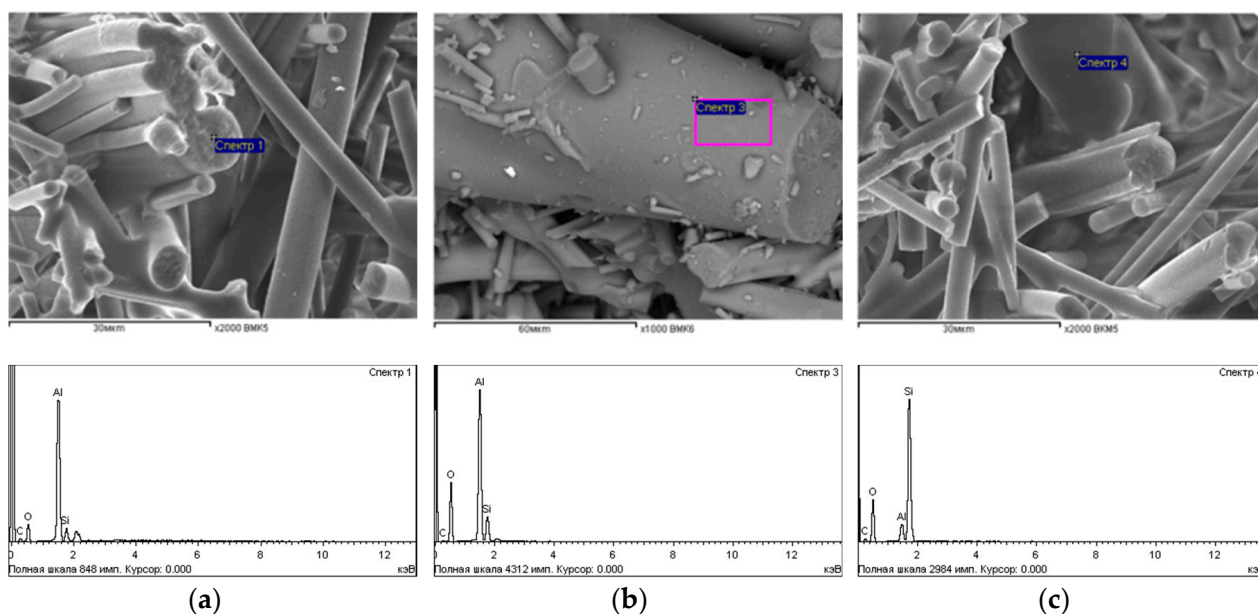


Figure 9. Micrographs indicating the areas and points of EDS as well as the corresponding spectra: (a) skeleton fibers, the material II; (b) skeleton fibers, the material I; (c) the area of fiber fusion (the fusion mode), the material I.

3.4. Compressive Strength

The average value of the compressive strength for the initial material I is 11 MPa. In general, treatment of the material with concentrated solar radiation does not lead to a decrease in strength. The fracture pattern and the shape of the load-elongation curve have no fundamental differences. At the same time, the strength of specimens cut from different parts of the treated material I is somewhat different (Figure 10). The average values of the compressive strength of the specimens cut from the “cold” and “hot” sides are 9.6 and 10.7 MPa, respectively. This may also indicate changes in the structure of the material. The average value of the compressive strength for the initial material II is about 1.5 MPa. After exposure to concentrated solar radiation, the strength decreases to 0.6 MPa. The compressive strength for the initial material III is at the level of 0.4–0.6 MPa. With prolonged heating by solar radiation, as in the previous case, degradation of properties is noticeable. In some cases, delamination was observed on the “cold” side of the material III specimens.

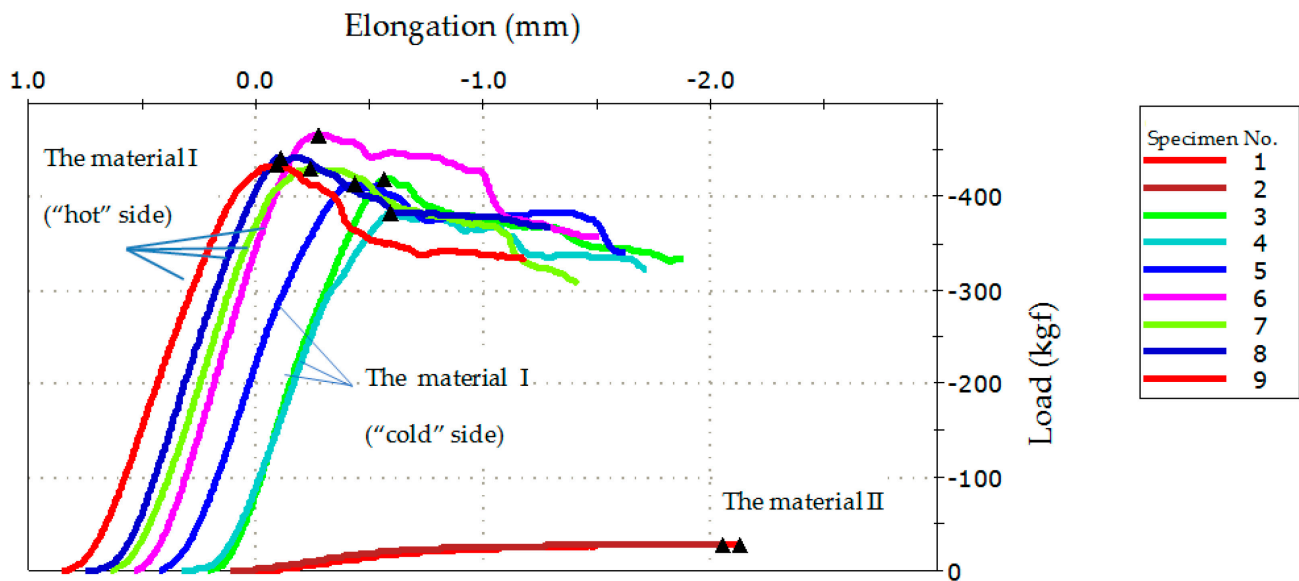


Figure 10. The load-elongation curves for compression testing for the materials I, II.

4. Conclusions

The phase composition, microstructure, elemental composition, and mechanical properties of three heat-insulating ceramic fibrous materials of the Al_2O_3 - SiO_2 system, characterized by different densities, have been studied after prolonged exposure to concentrated solar radiation. It has been shown in the study that the investigated materials retain their fibrous structure under prolonged treatment in the first mode up to temperatures of 1600 °C. The phase composition of the processed ceramic materials changes, and with a decrease in the density of the material, the changes are more pronounced. The treatment of the material with a density of 1000 kg/m^3 (the material I) leads to the formation of a new phase component—corundum (α - Al_2O_3). It is more likely that this can be associated with the transition of the initial metastable phase δ - Al_2O_3 to the stable α - Al_2O_3 than with the formation of phases from the initial mullite. An increased amount of α - Al_2O_3 is observed on the surface of the “hot” side sample. The mechanical properties of the material I are slightly reduced as a result of exposure to concentrated solar radiation. The average values of the compressive strength of the specimens cut from the “cold” and “hot” sides are 9.6 and 10.7 MPa, respectively. The treatment of the material with a density of 500 kg/m^3 (the material II) leads to the formation of another phase component (in addition to corundum)—cristobalite (SiO_2). It probably forms from an amorphous binder. A change in the structure of the material II leads to a decrease in strength from 1.5 to 0.6 MPa. The material with a density of 300 kg/m^3 (the material III) also contains corundum and cristobalite after prolonged heating. In some cases, delamination of the material III is observed.

The treatment of all three materials in the fusion mode results in the formation of the eutectic component in the form of spherulites.

It is stated that the material I, with a density of 1000 kg/m^3 , is the most resistant to high-speed heating by concentrated solar radiation. The greatest structural changes are observed for the materials with a lower density (the materials II, III). The effective operating temperature of such materials should not exceed 1600 °C.

Author Contributions: Conceptualization, V.G.B. and S.Kh.S.; Investigation, V.G.B., S.Kh.S. and Y.V.S.; Methodology, V.G.B. and S.Kh.S.; Project administration, V.G.B.; Supervision, V.G.B.; Visualization, E.A.S.; Writing—original draft, E.A.S. and Y.V.S.; Writing—review & editing, M.I.D. All authors have read and agreed to the published version of the manuscript.

Funding: This research was funded by the ministry of science and higher education of the Russian federation, agreement No. 075-11-2021-077.

Institutional Review Board Statement: Not applicable.

Informed Consent Statement: Not applicable.

Data Availability Statement: Data sharing is not applicable to this article.

Conflicts of Interest: The authors declare no conflict of interest.

References

1. Mittenbühler, A.; Jung, J. Ceramic materials under high temperature heat transfer conditions. *J. Nucl. Mater.* **1990**, *171*, 54–62. [[CrossRef](#)]
2. Chen, H.; Sui, X.; Zhou, C.; Wang, C.; Yin, C.; Liu, F. Preparation and characterization of mullite fiber-reinforced Al₂O₃-SiO₂ aerogel composites. *Key Eng. Mater.* **2015**, *697*, 360–363. [[CrossRef](#)]
3. Wen, S.; Ren, H.; Zhu, J.; Bi, Y.; Zhang, L. Fabrication of Al₂O₃ aerogel-SiO₂ fiber composite with enhanced thermal insulation and high heat resistance. *J. Porous Mater.* **2019**, *26*, 1027–1034. [[CrossRef](#)]
4. Wen, S.; Zhu, J.; Yin, Q.; Bi, Y.; Ren, H.; Zhang, L. Fabrication of infrared opacifiers loaded Al₂O₃ aerogel-SiO₂ fiber mat composites with high thermal resistance. *Int. J. Nanosci.* **2020**, *19*, 1950021. [[CrossRef](#)]
5. Li, C.-H.; Hu, L.; Zou, Y.; Liu, J.-A.; Xiao, J.-H.; Wu, J.-M.; Shi, Y.-S. Fabrication of Al₂O₃-SiO₂ ceramics through combined selective laser sintering and SiO₂-sol infiltration. *Int. J. Appl. Ceram. Technol.* **2020**, *17*, 255–263. [[CrossRef](#)]
6. Liu, M.; Liu, J.; Wang, M.; Yun, Z. Preparation and properties of SiO₂/Al₂O₃-SiO₂ fiber mat composite materials. *Key Eng. Mater.* **2016**, *680*, 129–132. [[CrossRef](#)]
7. Chen, Y.T.; Chong, K.K.; Lim, C.S.; Lim, B.H.; Tan, K.K.; Aliman, O.; Bligh, T.P.; Tan, B.K.; Ismail, G. Report of the first prototype of non-imaging focusing heliostat and its application in high temperature solar furnace. *Sol. Energy* **2002**, *72*, 531–544. [[CrossRef](#)]
8. Fend, T.; Hoffschmidt, B.; Pitz-Paal, R.; Reutter, O.; Rietbrock, P. Porous materials as open volumetric solar receivers: Experimental determination of thermophysical and heat transfer properties. *Energy* **2004**, *29*, 823–833. [[CrossRef](#)]
9. Pierrat, B.; Balat-Pichelin, M.; Silvestroni, L.; Sciti, D. High temperature oxidation of ZrC-20%MoSi₂ in air for future solar receivers. *Sol. Energy Mater. Sol. Cells* **2011**, *95*, 2228–2237. [[CrossRef](#)]
10. Paizullakhanov, M.S.; Faiziev, S.A.; Nurmatov, S. Studying refractoriness of silicon-carbide materials fabricated in a Big Solar Furnace. *Appl. Sol. Energy* **2007**, *43*, 268–269. [[CrossRef](#)]
11. Lugovoy, A.A.; Babashov, V.G.; Karpov, U.V. The thermal diffusivity of the gradient thermal insulation material. *Tr. VIAM (Proc. VIAM)* **2014**, *2*, 1–10. [[CrossRef](#)]
12. Vlasova, M.; Kakazey, M.; Castro Hernandez, A.; Márquez Aguilar, P.A.; Guardian Tapia, R.; Mel'nikov, I.V.; Petrovsky, V.N. Surface changes in Al₂O₃-base composite ceramics under action of laser treatment. *Ceram. Int.* **2019**, *45*, 5454–5466. [[CrossRef](#)]
13. Cappelli, E.; Orlando, S.; Sciti, D.; Montozzi, M.; Pandolfi, L. Ceramic surface modifications induced by pulsed laser treatment. *Appl. Surf. Sci.* **2000**, *154–155*, 682–688. [[CrossRef](#)]
14. Suleimanov, S.K.; Babashov, V.G.; Dzhanklich, M.U.; Dyskin, V.G.; Daskovskii, M.I.; Skripachev, S.Y.; Kulagina, N.A.; Arushanov, G.M. Behavior of a heat-protective material based on Al₂O₃ and SiO₂ fibers under exposure to concentrated solar energy flux. *Refract. Ind. Ceram.* **2021**, *61*, 675–679. [[CrossRef](#)]
15. Babashov, V.G.; Suleimanov, S.K.; Skripachev, S.Y.; Basargin, O.V.; Lyulyukina, G.Y. Phase transformations in high-temperature fiber materials exposed to non-equilibrium flow of heat and light. *Glass Ceram.* **2020**, *76*, 374–380. [[CrossRef](#)]